

Model Compression for DNN-Based Speaker Verification Using Weight Quantization

Jingyu Li¹, Wei Liu¹, Zhaoyang Zhang¹, Jiong Wang², Tan Lee¹

¹Department of Electronic Engineering, The Chinese University of Hong Kong, Hong Kong

²School of Science and Engineering, The Chinese University of Hong Kong, Shenzhen, China

{lijingyu0125, louislau.1129, zhaoyangzhang}@link.cuhk.edu.hk, jiongwang@link.cuhk.edu.cn, tanlee@ee.cuhk.edu.hk

Abstract

DNN-based models achieve significant performance in the speaker verification (SV) task with substantial computation costs. Model compression can be applied to reduce the model size for lower resource consumption. The present study exploits weight quantization to compress two widely-used SV models, ECAPA-TDNN and ResNet. The experiments on VoxCeleb indicate that quantization is effective for compressing SV models, where the model size can be reduced by multiple times with no noticeable performance decline. ResNet achieves more robust results than ECAPA-TDNN using lower-bitwidth quantization. The analysis of layer weights shows that the smooth distribution of ResNet may contribute to its robust results. The additional experiments on CN-Celeb validate the quantized model's generalization ability in the language mismatch scenario. Furthermore, information probing results demonstrate that the quantized models can preserve most of the learned speaker-relevant knowledge compared to the original models.

Index Terms: speaker verification, weight quantization, model compression, cross languages, information probe

1. Introduction

Speaker verification (SV) is a biometric authentication process verifying whether a spoken utterance is from the claimed speaker [1, 2]. Deep learning network (DNN) models have shown great success in SV [3–8] and outperformed conventional methods, e.g., I-vector [9]. Despite significant performance gain attained with these DNN models, it comes at the cost of higher computation complexity. SV systems are expected to be run locally on devices without Internet connections [10]. In these scenarios, offline processing (as opposed to online processing from the cloud) offers some advantages. The problem of Internet transmission delays can be mitigated. Users' private data are kept safe without being exposed outside the device. However, the computation cost of current DNN-based SV systems does not allow them to run on these resource-constrained devices.

To reduce the required resource consumption, model compression is expected. The capability of the compressed model should remain consistent with the original model. Various compression methods, such as weight quantization [11–14], pruning [15, 16], and knowledge distillation [17], have been studied on different tasks [18, 19]. The present study focuses on the method of weight quantization for DNN-based speaker embedding extraction models. The default data bitwidth used in existing deep learning frameworks is 32, e.g., PyTorch [20] and TensorFlow [21]. The core operation in model compression by weight quantization is mapping full-bitwidth model weights

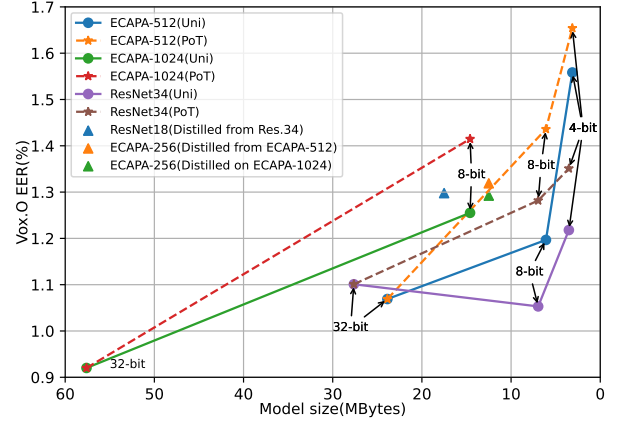


Figure 1: Model Size vs. Vox.O EER(%), lower is better. Uni stands for uniform quantization, and PoT stands for Powers-of-Two. The quantization bitwidth is annotated alongside the nodes.

onto a lower-bitwidth representation, which reduces the model size and enables faster processing.

To the best of our knowledge, weight quantization has not been investigated on state-of-the-art DNN SV models. ECAPA-TDNN [7] and ResNet [5, 6, 22] are two widely-used well-performing models for speaker embedding extraction. Many SV models have been developed based on them [8, 23, 24]. In this study, we apply weight quantization to these two models. The experiments are carried out with the VoxCeleb datasets [6, 25, 26], with two common quantization methods: learnable uniform quantization [27] and Powers-of-Two quantization [28]. Our preliminary experiments show that weight quantization is effective for SV model compression. With multiple times smaller sizes than the original models, the performance of quantized ECAPA and ResNet declines slightly, as shown in Fig. 1. ResNet's results are more robust than ECAPA, especially in 4-bit quantization. To investigate the cause of such a difference, we analyzed the distribution of layer weights of these two models. The highly concentrated weight distribution of ECAPA is observed, which may explain its larger performance decline than ResNet using lower-bitwidth quantization. This also provides several empirical guidelines for weight quantization. As reducing the model size, the learning ability of the quantized model is decreased compared to the original counterpart. The poorer learning ability may affect the models' generalization ability and extracted knowledge. We evaluate the generalization of quantized models using a language-mismatch SV test, which is performed on CN-Celeb without model fine-tuning.

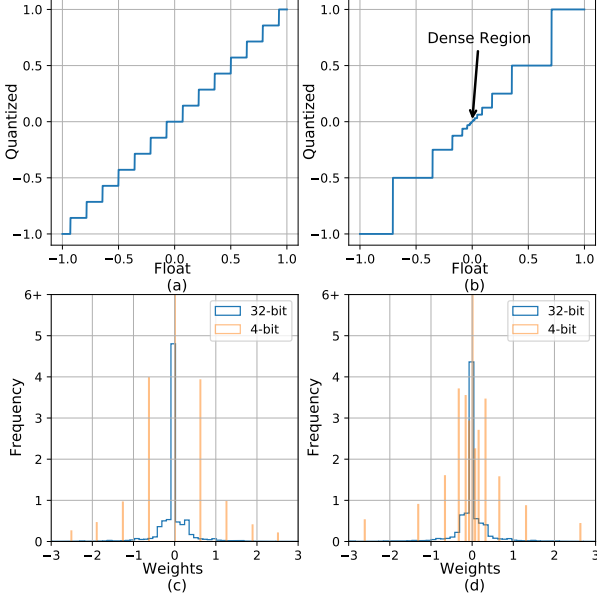


Figure 2: The quantization levels of (a) uniform and (b) PoT quantization. The weights distribution of 32-bit weights and 4-bit quantized by (c) uniform, (d) PoT.

The extracted knowledge is investigated on the speaker embeddings before and after model quantization using four information probe tasks.

The paper is organized as follows: Section 2 introduces the details of the quantization methods. The experimental setting and results are given in Sections 3 and 4, respectively. Finally, we give a brief conclusion in Section 5.

2. Quantization

A trainable weight in a layer is denoted as $\mathcal{W} \in \mathbb{R}^N$. In a convolutional layer (CNN), $N = h \times w \times c_1 \times c_2$. In a fully-connected layer (FC), $N = c_1 \times c_2$. \mathcal{W} takes continuous values. The quantization of \mathcal{W} is expressed as

$$\widehat{\mathcal{W}} = \Gamma(\lfloor \mathcal{W}, \alpha \rfloor)_{\mathbf{q}(\alpha, b)} \quad (1)$$

\mathcal{W} is first normalized by its mean and standard deviation so that it can be represented in a symmetric range. They are clipped into a range of $[-\alpha, \alpha]$ by a function denoted as $\lfloor \cdot, \alpha \rfloor$, where $\alpha (\geq 0)$ is a learnable parameter. $\Gamma(\cdot)_{\mathbf{q}}$ represents a projection function, mapping continuous values into a set of discrete values $\mathbf{q} = [\pm q_1, \pm q_2, \dots, \pm q_{\frac{n}{2}}]$. $n = 2^b$ is the number of quantization levels. b is the bitwidth and is usually pre-determined. The quantization level, i.e., the values of $[q_1, q_2, \dots]$, is another critical factor determining the performance of the quantized models. Uniform and Powers-of-Two quantization are widely used [27–31] for constructing the quantization level. They are easy to implement and friendly to both software and hardware implementations.

2.1. Uniform Quantization

The quantization levels of uniform quantization are represented as

$$\mathbf{q}(\alpha, b) = [0, \frac{\pm 1}{2^{b-1}-1}, \frac{\pm 2}{2^{b-1}-1}, \dots, \pm 1] \times \alpha \quad (2)$$

Uniform quantization generates the discrete values uniformly along $[-1, 1]$, as illustrated in Fig. 2(a). The length of each quantization step is constant, i.e., $\frac{1}{2^{b-1}-1}$. A smaller step length gives denser discrete levels to distinguish different values. However, the distribution of weights is usually non-uniform [15]. For instance, a layer’s weight distribution from a trained model is plotted by the blue curve in Fig. 2(c). There are more weights concentrated around the center and fewer weights around the boundaries. The orange line in Fig. 2(c) shows the uniform quantization level. The minor numerical differences between weights are erased if they lie in the same quantization level. Thus a large proportion of the weights around the center will be assigned to an identical value, which may dramatically degrade the model performance.

2.2. Powers-of-Two Quantization

The quantization levels of Powers-of-Two (PoT) quantization are represented as

$$\mathbf{q}(\alpha, b) = [0, \pm 2^{-2^{b-1}+2}, \dots, \pm 2^{-1}, \pm 1] \times \alpha \quad (3)$$

PoT provides non-identical discrete levels, unlike uniform quantization, as shown in Fig. 2(b). The quantization levels around the center are denser. The denser levels provide a more refined quantization description of weight parameters, as shown by the orange lines in Fig. 2(d). Sparser quantization levels are proposed near the boundary. If only a few weights lie around the boundary, as in Fig. 2(d), discretizing the weights will not significantly affect the quantization error.

2.3. Parameter Update

The quantization error ($\|\mathcal{W} - \widehat{\mathcal{W}}\|^2$) depends heavily on the value of α . A large α covers a wide range of weight values, and the quantization levels are distributed sparsely. A smaller value of α gives denser discrete levels, and more weights will be clipped to $-\alpha$ or α , resulting in higher quantization errors. The distributions of weights in different layers are not identical, and a constant clipping value may not be optimal for quantizing \mathcal{W} . In this paper, α is made learnable as in [12]. Each layer is assigned an α , and the value of α is updated during model training by backward propagation. $\lfloor \cdot, \alpha \rfloor$ and $\Gamma(\cdot)_{\mathbf{q}}$ are two discrete operations, where the gradients cannot be calculated directly. Following [13], the gradients for α and \mathcal{W} are estimated by Straight-Through Estimator (STE) [32] as

$$\frac{\partial \mathcal{L}}{\partial \alpha} = \frac{\partial \mathcal{L}}{\partial \widehat{\mathcal{W}}} \frac{\partial \widehat{\mathcal{W}}}{\partial \alpha}, \quad \frac{\partial \widehat{\mathcal{W}}}{\partial \alpha} = \begin{cases} \text{sign}(\mathcal{W}) & \text{if } |\mathcal{W}| > \alpha \\ \frac{\widehat{\mathcal{W}}}{\alpha} - \frac{\mathcal{W}}{\alpha} & \text{if } |\mathcal{W}| \leq \alpha \end{cases} \quad (4)$$

$$\frac{\partial \mathcal{L}}{\partial \mathcal{W}} = \frac{\partial \mathcal{L}}{\partial \widehat{\mathcal{W}}} \frac{\partial \widehat{\mathcal{W}}}{\partial \mathcal{W}}, \quad \frac{\partial \widehat{\mathcal{W}}}{\partial \mathcal{W}} = 1 \quad (5)$$

where \mathcal{L} is the training loss. In each training step, the full-precision \mathcal{W} is first converted into $\widehat{\mathcal{W}}$ with discrete values. $\widehat{\mathcal{W}}$ is used for the computational process, such as convolution or matrix multiplication. Thus the calculation of $\frac{\partial \mathcal{L}}{\partial \mathcal{W}}$ can be performed as the conventional gradient computation. After training, the \mathcal{W} is quantized to $\widehat{\mathcal{W}}$ and stored. In the inference, the model is processed using the $\widehat{\mathcal{W}}$, which requires less storage and computation cost.

Table 1: *Performances of the models. Vox.O, Vox.E, Vox.H are short for the Original, Easy and Hard test sets of Vox.1*

Model	Parameters (M)	MACs (Giga)	Compression	Bitwidth (bits)	Size (MBytes)	EER(%)		
						Vox.O	Vox.E	Vox.H
ECAPA-TDNN-512	5.95	0.96	-	32	23.87	1.07	1.28	2.43
			Uni	8	6.09	1.20	1.46	2.75
			PoT			1.43	1.69	3.11
			Uni	4	3.13	1.56	1.78	3.29
			PoT			1.65	1.86	3.41
ECAPA-TDNN-1024	14.38	2.56	-	32	57.61	0.92	1.15	2.28
			Uni	8	14.6	1.26	1.45	2.73
			PoT			1.41	1.59	2.99
ResNet34	6.9	3.67	-	32	27.63	1.10	1.15	2.08
			Uni	8	6.96	1.05	1.11	2.02
			PoT			1.28	1.34	2.41
			Uni	4	3.52	1.22	1.29	2.32
			PoT			1.35	1.40	2.52
ECAPA-TDNN-256	3.11	0.43	-	32	12.5	1.43	1.59	2.87
			distill(512)			1.29	1.53	2.88
			distill(1024)			1.30	1.53	2.85
ResNet18	4.37	1.78	-	32	17.51	1.45	1.44	2.53
			distill			1.33	1.39	2.48

3. Experimental set-up

3.1. Datasets

The datasets utilized in the experiments are VoxCeleb 1&2 (Vox.1 & Vox.2) [6,25,26]. Speech data in VoxCeleb are mostly in English. The development set of Vox.2 consists of 5,994 speakers and is used for model training. Vox.1 is used to evaluate the performance of models. Three test sets are constructed using data from Vox.1 and denoted as Original, Easy, and Hard sets, respectively.

In addition, the test set of CN-Celeb [33] is used to evaluate the models' performance in another language. CN-Celeb is a large-scale Chinese dataset consisting of about 1,000 speakers.

3.2. Model training and evaluation

ECAPA-TDNN with 512 and 1024 channels, ResNet34 with 32 channels are experimented with. The training process consists of two stages. The model is first trained in full precision, i.e., float32 in PyTorch. The model is trained to predict the input speaker identity using the additive angular margin softmax (AAM-softmax) [34] as the classification loss. The margin and scale of AAM-softmax are set to be 0.2 and 30. The Adam optimizer [35] with a weight decay of $2e-5$ is utilized for training the model. The learning rate is initialized as 0.001 and decayed by a ratio of 0.1 at the 20th and 32nd epoch, respectively. The whole training process consists of 40 epochs. In each training step, 128 utterances are randomly sampled from the training set, and a 2-second long segment is cropped from each input randomly. The model input is 64-dimensional *log* Mel-filterbanks (FBanks) transformed from the raw waveform of each segment using the hamming window. The window size is 25ms, and the hop length equals 10ms. Background sound addition and audio reverberation are utilized for data augmentation in training. Background sounds are randomly selected from MUSAN [36]. The simulated room impulse responses sampled from [37] are utilized for audio reverberation.

In the second stage, the quantized model is fine-tuned from

Table 2: *Performances of the models on CN-Celeb*

Model	Compression	EER(%)
ECAPA-TDNN-512	-	17.61
	Uni,8-bit	17.50
	Uni,4-bit	16.12
ResNet34	-	11.85
	Uni,8-bit	11.75
	Uni,4-bit	11.93
ECAPA-TDNN-256	distill(512)	18.13
	distill(1024)	18.17
ResNet18	distill	12.32

the previously trained full-precision model for 20 epochs. The learning rate is reduced by a ratio of 0.1 at the 10th and 16th epochs. Reducing the model size decreases the learning ability, thus data augmentation is not used for training the quantized models. The rest of the training settings remain the same for the full-precision model.

For evaluation, each utterance is evenly cropped into 4-second long segments, with a 1-second overlap between two adjacent segments. The cosine similarity values between the test utterance segments and the enrollment segments are averaged as the verification score. Adaptive s-norm (AS-norm) [38] is applied to calibrate the scores. The performance is reported in terms of equal error rate (EER).

4. Results and Analysis

4.1. Learnable quantization

The model results on the three test sets of Vox.1 are shown in Table 1. The model computation complexity is represented by the number of multiply-accumulate operations (MACs). The 8-bit quantization reduces the model size by around 4 times. Uniform quantization shows slightly better results than PoT.

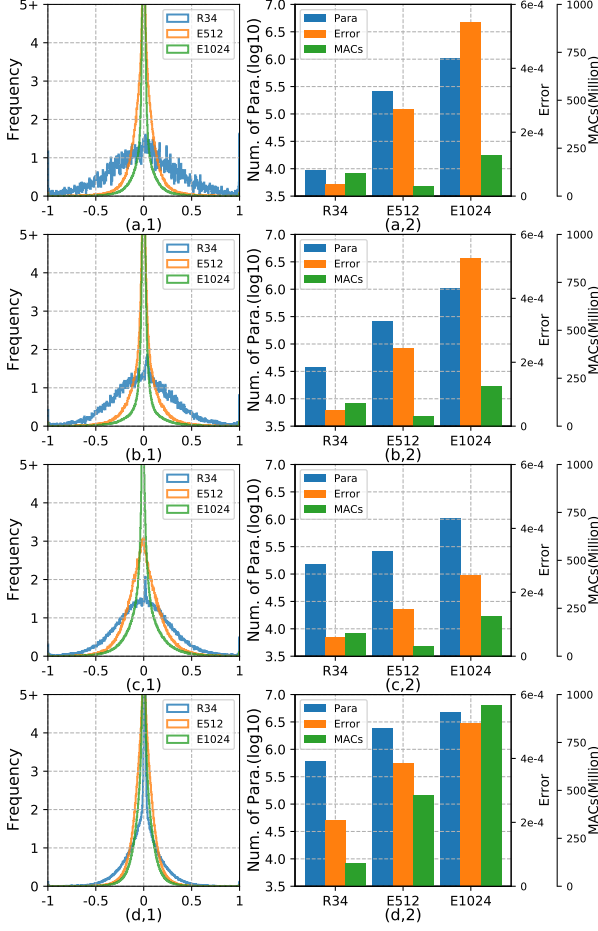


Figure 3: The weight distributions are shown in (a,1) to (d,1). R34 stands for ResNet34, E512 for ECAPA-512, and E1024 for ECAPA-1024. (a,2) to (d,2) gives the number of parameters, averaged quantization error, and MACs of layers.

The performance of ECAPA-TDNN-512 is declined by around 15% in all three test sets. The ECAPA-1024 has the same structure as ECAPA-512 and doubles the convolution channel size, which increases the model complexity. ECAPA-1024 outperforms ECAPA-512 in full precision but gives close results in the 8-bit uniform-quantized models. ResNet gives more robust results than ECAPA. The performance of ResNet34 is almost not degraded by uniform quantization in all three test sets, and PoT gives around a 15% increase in EER.

Lower bitwidth is evaluated on ECAPA-512 and ResNet34. The 4-bit quantization reduces the model size by about 8 times. The EERs of 4-bit ECAPA-512 are increased by about 50% compared with the full-precision model. The decline of ResNet34’s performance is 10 to 20%, which is significantly less than that of ECAPA-512. ResNet34 has a model size close to ECAPA-512, but its MACs are much larger than ECAPA’s, which may contribute to its minor performance degradation.

4.2. Weight analysis

Several layers’ weight distribution and statistics information are given in Fig. 3. These models are uniform-quantized using 8-bit. The last convolution layers of Block 1 to 4 of ResNet34 are

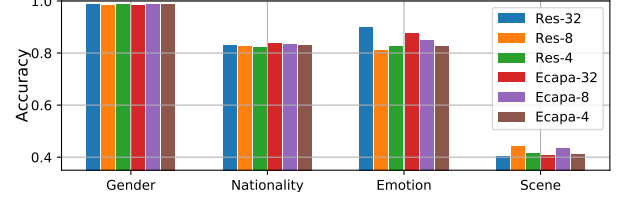


Figure 4: Accuracy of probing tasks for models with different bitwidths. Res-32 is short for ResNet34 with 32-bit, Ecapa-8 for ECAPA-512 with 8-bit, etc.

given in (a)-(d), respectively. For ECAPA structures, the last convolution layers of Block 1 to 3, and the convolution layer before attentive statistics pooling are shown. The weights are clipped by the corresponding α and scaled into $[-1, 1]$ for better visualization. “Error” denotes the averaged quantization error of the corresponding layer.

Among the three models, the weight distributions of the ECAPA networks are highly concentrated, and ResNet34’s distributions show smoother bell shapes. The distribution of ResNet also becomes sharper as the number of parameters increases, as shown in Fig. 3(d). It can be observed that the averaged quantization error is positively related to the number of parameters in a layer, indicating that it is challenging to quantize the layers with a large number of parameters. The parameters are evenly distributed among layers in the same block of ResNet34, whereas the parameters concentrate densely on a block’s first and last convolution layers in the ECAPA structure. The dense layers of ECAPA may explain its larger quantization performance decline compared to ResNet. This suggests an empirical guideline for model design is to avoid concentrating a large number of parameters on several layers.

4.3. Evaluation on CN-Celeb

The models trained on VoxCeleb are evaluated on this dataset without fine-tuning to evaluate their generalization ability in a different language. The results are summarized in Table 2. Interestingly, the 8-bit quantized model shows superior performance to the full-precision model on ECAPA-512, and the 4-bit model gives the lowest EER. ResNet34 outperforms ECAPA-512 with or without the quantization, indicating it has a better generalization ability. The 8-bit quantized ResNet34 also outperforms its original model. There is a slight performance drop on the 4-bit ResNet34. [13] found that quantization may contribute to weight regularization, which can alleviate the overfitting problem of the full-precision model. This effect may increase the model generalization in cross-language SV.

4.4. Compared with distillation

We compare the quantized models with models compressed in another method, i.e., knowledge distillation. The model distillation is performed on two smaller networks, ECAPA-TDNN-256 and ResNet18. ECAPA-256 is constructed by using 256 convolution channels. Three training settings are performed on all models. The distillation loss is calculated at the speaker embedding level by \mathcal{L}_2 loss. As shown in Table 1, the distilled models give around 10% lower EER than the model trained from scratch on all three test sets. The performance gap between ECAPA 512-distilled and 1024-distilled is small. Compared with the models compressed by distillation, the 8-bit quantized ECAPA structure uses a half size and gives a close performance.

The quantized ResNet uses a smaller size and achieves superior performance to its distilled variant. The results on CN-Celeb, given in Table 2, show that the quantized models are more robust than those compressed by distillation.

4.5. Information probe

Information probing tasks are conducted on the speaker embeddings extracted by the original and quantized models. Four classification tasks are applied, i.e., nationality, gender, emotion, and scene. The first two tasks are trained on Vox.2 and evaluated on Vox.1. SAVEE [39] is used for the emotion classification, and TAU Urban Acoustic Scenes 2020 Mobile [40] for scene classification. A multi-layer perceptron with two FC layers and ReLU activation is utilized as the classifier.

The results are summarized in Fig. 4. The accuracy of gender classification is over 98% for all models, indicating that the quantization does not affect this information much. Nationality and emotion are two factors related to the speakers' speaking styles, e.g., accents and pitches. The classifiers achieve accuracy higher than 80% on both tasks for all models. The accuracy is decreased slightly in quantized models compared to the full-size models. The scene classification accuracy is observably lower than other tasks. However, the quantized models show higher accuracy in this task than the original models. The environmental sounds may have biases for different speakers. The quantized models can rely on biased environment information for distinguishing speakers, but this effect will cause more errors in SV under noisy environments. The full-size model may have a stronger learning ability to depress the disturbance from environmental information.

5. Conclusions and future work

This paper exploits weight quantization to compress DNN-based SV models. The experiments are carried out on two commonly-used SV model structures: ECAPA and ResNet. The experiments show that the SV model size can be compressed by multiple times with a slight performance decline. The ResNet gives robust performance after quantization. The performance of ECAPA is affected more by low-bitwidth quantization than ResNet. The quantized models perform comparable or better than the full-precision models in a cross-language SV evaluation, indicating that the model's generalization ability is preserved after model quantization. The quantized models retain the speaker-relevant knowledge and obtain additional information with respect to the environmental sound.

6. Acknowledgements

The first author was supported by the Hong Kong PhD Fellowship Scheme.

7. References

- [1] J. P. Campbell, "Speaker recognition: A tutorial," *Proceedings of the IEEE*, vol. 85, no. 9, pp. 1437–1462, 1997.
- [2] Z. Wu, N. Evans, T. Kinnunen *et al.*, "Spoofing and countermeasures for speaker verification: A survey," *speech communication*, vol. 66, pp. 130–153, 2015.
- [3] D. Snyder, D. Garcia-Romero, G. Sell, D. Povey, and S. Khudanpur, "X-vectors: Robust dnn embeddings for speaker recognition," in *ICASSP 2018*. IEEE, 2018, pp. 5329–5333.
- [4] W. Xie, A. Nagrani, J. S. Chung, and A. Zisserman, "Utterance-level aggregation for speaker recognition in the wild," in *ICASSP 2019*. IEEE, 2019, pp. 5791–5795.
- [5] H. S. Heo, B.-J. Lee, J. Huh *et al.*, "Clova baseline system for the voxceleb speaker recognition challenge 2020," *arXiv preprint arXiv:2009.14153*, 2020.
- [6] A. Nagrani, J. S. Chung, and A. Zisserman, "Voxceleb: A large-scale speaker identification dataset," *Interspeech*, pp. 2616–2620, 2017.
- [7] B. Desplanques, J. Thienpondt, and K. Demuynck, "Ecapa-tdnn: Emphasized channel attention, propagation and aggregation in tdnn based speaker verification," *Interspeech*, pp. 3830–3834, 2020.
- [8] J. Thienpondt, B. Desplanques, and K. Demuynck, "Integrating Frequency Translational Invariance in TDNNs and Frequency Positional Information in 2D ResNets to Enhance Speaker Verification," in *Interspeech*, 2021, pp. 2302–2306.
- [9] N. Dehak, P. J. Kenny, R. Dehak, P. Dumouchel, and P. Ouellet, "Front-end factor analysis for speaker verification," *IEEE Transactions on Audio, Speech, and Language Processing*, vol. 19, no. 4, pp. 788–798, 2010.
- [10] J. Kim, S. Chang, and N. Kwak, "PQK: model compression via pruning, quantization, and knowledge distillation," in *Interspeech*. ISCA, 2021, pp. 4568–4572.
- [11] S. Zhou, Y. Wu, Z. Ni *et al.*, "Dorefa-net: Training low bitwidth convolutional neural networks with low bitwidth gradients," *arXiv preprint arXiv:1606.06160*, 2016.
- [12] J. Choi, Z. Wang, S. Venkataramani *et al.*, "Pact: Parameterized clipping activation for quantized neural networks," *arXiv preprint arXiv:1805.06085*, 2018.
- [13] Y. Li, X. Dong, and W. Wang, "Additive powers-of-two quantization: An efficient non-uniform discretization for neural networks," in *ICLR*, 2020.
- [14] Z. Zhang, W. Shao, J. Gu, X. Wang, and P. Luo, "Differentiable dynamic quantization with mixed precision and adaptive resolution," in *ICML*, vol. 139, 2021, pp. 12 546–12 556.
- [15] S. Han, H. Mao, and W. J. Dally, "Deep compression: Compressing deep neural networks with pruning, trained quantization and Huffman coding," *arXiv preprint arXiv:1510.00149*, 2015.
- [16] H. Li, A. Kadav, I. Durdanovic *et al.*, "Pruning filters for efficient convnets," in *ICLR*, 2017.
- [17] A. Polino, R. Pascanu, and D. Alistarh, "Model compression via distillation and quantization," in *ICLR*, 2018.
- [18] A. D. A. Salvi and R. C. Barros, "Model compression in object detection," in *2021 International Joint Conference on Neural Networks (IJCNN)*. IEEE, 2021, pp. 1–8.
- [19] Y. Cheng, D. Wang, P. Zhou, and T. Zhang, "Model compression and acceleration for deep neural networks: The principles, progress, and challenges," *IEEE Signal Processing Magazine*, vol. 35, no. 1, pp. 126–136, 2018.
- [20] A. Paszke, S. Gross, F. Massa *et al.*, "Pytorch: An imperative style, high-performance deep learning library," in *NeurIPS*, 2019, pp. 8024–8035.
- [21] M. Abadi, A. Agarwal, P. Barham *et al.*, "TensorFlow: Large-scale machine learning on heterogeneous systems," 2015, software available from tensorflow.org. [Online]. Available: <https://www.tensorflow.org/>
- [22] K. He, X. Zhang, S. Ren *et al.*, "Deep residual learning for image recognition," in *CVPR*, 2016, pp. 770–778.
- [23] T. Liu, R. K. Das, K. A. Lee, and H. Li, "MFA: TDNN with multi-scale frequency-channel attention for text-independent speaker verification with short utterances," in *ICASSP*. IEEE, 2022, pp. 7517–7521.
- [24] J. Li and T. Lee, "Text-independent speaker verification with dual attention network," *Interspeech*, pp. 956–960, 2020.
- [25] J. S. Chung, A. Nagrani, and A. Zisserman, "Voxceleb2: Deep speaker recognition," *Interspeech*, pp. 1086–1090, 2018.

- [26] A. Nagrani, J. S. Chung, W. Xie, and A. Zisserman, "Voxceleb: Large-scale speaker verification in the wild," *Computer Science and Language*, 2019.
- [27] Z. Cai, X. He, J. Sun, and N. Vasconcelos, "Deep learning with low precision by half-wave gaussian quantization," in *CVPR*, 2017, pp. 5918–5926.
- [28] A. Zhou, A. Yao, Y. Guo *et al.*, "Incremental network quantization: Towards lossless cnns with low-precision weights," in *ICLR*, 2017.
- [29] R. Gong, X. Liu, S. Jiang, T. Li, P. Hu, J. Lin, F. Yu, and J. Yan, "Differentiable soft quantization: Bridging full-precision and low-bit neural networks," in *Proceedings of the IEEE/CVF International Conference on Computer Vision*, 2019, pp. 4852–4861.
- [30] D. Miyashita, E. H. Lee, and B. Murmann, "Convolutional neural networks using logarithmic data representation," *arXiv preprint arXiv:1603.01025*, 2016.
- [31] A. Gholami, S. Kim, Z. Dong, Z. Yao, M. W. Mahoney, and K. Keutzer, "A survey of quantization methods for efficient neural network inference," *arXiv preprint arXiv:2103.13630*, 2021.
- [32] Y. Bengio, N. Léonard, and A. Courville, "Estimating or propagating gradients through stochastic neurons for conditional computation," *arXiv preprint arXiv:1308.3432*, 2013.
- [33] Y. Fan, J. Kang, L. Li *et al.*, "Cn-celeb: a challenging chinese speaker recognition dataset," in *ICASSP*. IEEE, 2020, pp. 7604–7608.
- [34] J. Deng, J. Guo, N. Xue, and S. Zafeiriou, "Arcface: Additive angular margin loss for deep face recognition," in *CVPR*, 2019, pp. 4690–4699.
- [35] D. P. Kingma and J. Ba, "Adam: A method for stochastic optimization," in *ICLR*, 2015.
- [36] D. Snyder, G. Chen, and D. Povey, "Musan: A music, speech, and noise corpus," *arXiv preprint arXiv:1510.08484*, 2015.
- [37] T. Ko, V. Peddinti, D. Povey *et al.*, "A study on data augmentation of reverberant speech for robust speech recognition," in *ICASSP*. IEEE, 2017, pp. 5220–5224.
- [38] P. Matejka, O. Novotný, O. Plchot *et al.*, "Analysis of score normalization in multilingual speaker recognition," in *Interspeech*, 2017, pp. 1567–1571.
- [39] P. Jackson and S. Haq, "Surrey audio-visual expressed emotion (savee) database," *University of Surrey: Guildford, UK*, 2014.
- [40] T. Heittola, A. Mesaros, and T. Virtanen, "Acoustic scene classification in DCASE 2020 challenge: Generalization across devices and low complexity solutions," in *Proceedings of 5th the Workshop on Detection and Classification of Acoustic Scenes and Events 2020 (DCASE 2020), Tokyo, Japan (full virtual)*, 2020, pp. 56–60.